17th World Conference on Earthquake Engineering, 17WCEE
Sendai, Japan - September 13th to 18th 2020

STRUCTURAL OPTIMIZATION OF STACKED ROCKING SPINE SYSTEMS FOR NONLINEAR EARTHQUAKE RESPONSE

A. Martin[1], G. G. Deierlein[2]

[1] *Ph.D. Student, Department of Civil & Environmental Engineering, Stanford University, Stanford, CA 94305, amorym@stanford.edu*
[2] *Professor, Department of Civil & Environmental Engineering, Stanford University, Stanford, CA 94305, ggd@stanford.edu*

Abstract

Conventional earthquake-resistant structural systems are susceptible to structural damage during severe earthquakes, which can lead to high repair costs as well as indirect economic losses. Stacked rocking systems offer an attractive solution by concentrating nonlinear response in reliable energy-dissipation components while limiting the force and deformation demands in elastic spines (concrete walls or steel braced frames) between the articulated yielding components. The design of systems with multiple rocking is challenging due to the complex nonlinear earthquake response, resulting from higher mode effects and nonlinear redistribution of internal forces between the rocking planes. In this paper, a novel optimization framework is developed to determine the number, location and properties of nonlinear energy dissipating components in stacked rocking systems. The cost of the elastic spine is minimized, while limiting peak story drifts to a specified target. An optimization framework is proposed based on a modified version of the sequential linear programming (SLP) is used as the optimization algorithm. A high-rise building prototype of 20 stories with stacked rocking reinforced concrete walls is considered for this study. Due to the high computational cost of nonlinear dynamic analyses needed for the optimization, a ground motion selection routine is identified to predict the median response from a suite of 50 hazard-consistent ground motions. In order to validate the ground motion selection routine, a dual hinge optimization procedure is implemented for the 20-story building. The optimization yields important considerations on the nonlinear earthquake response of stacked rocking systems, especially the reduction of higher mode force demands through additional energy-dissipation hinges above the base. Drastic reduction in seismic demands are obtained considering two rocking hinges for the 20-story high-rise building with a reduction of 30% for story shear forces and 42% for overturning moment.

Keywords: structural optimization; rocking system; nonlinear dynamic analysis; high-rise building

1. Introduction

Rocking spine systems are innovative lateral force-resisting systems, demonstrating superior seismic performance through uplift at the base and self-centering by action of post-tensioning (PT) cables. The rocking spine, comprised of either steel braced frame [1], reinforced concrete (RC) wall [2] or even cross-laminated timber (CLT) walls [3], is designed to have sufficient capacity to remain elastic up to maximum considered earthquake (MCE) level demands. Inelastic deformations are confined to nonlinear dampers, either hysteretic (buckling restrained braces, steel butterfly shear fuses, metallic fiction sliders) or fluid viscous dampers. The seismic force demands on the rocking spine are attenuated by introducing a rocking plane at the base of the structure in combination with nonlinear dampers. However, single rocking spine systems are susceptible to higher mode effects, especially for slender buildings [4]. These higher mode effects lead to an amplification of the bending moment envelope above the base of the rocking system, and hence, a costly elastic rocking spine.

Stacked rocking spine systems, whereby additional articulated rocking hinges are introduced along the height of the building, are an attractive higher mode mitigation technique [5]. An example stacked rocking system with three articulated hinges is shown in **Fig.1**. The seismic force demands from higher modes are reduced by inserting multiple nonlinear rocking planes. Researchers have investigated the seismic performance of multi-level rocking systems considering RC walls [6], rocking braced frames [7] and timber wall segments [8]. Multiple rocking sections limit the higher mode effects on shear and moment amplifications, while maintaining code-prescribed drift limits and negligible residual drifts. Using a parametric study, a 2-segment controlled spine frame was deemed advantageous for high-rise buildings over 20 stories with greatly reduced base shear and acceptable interstory drifts [9]. Similar to multiple rocking sections, multi-level isolation have also been investigated as a seismic mitigation technique [10]. Mid-story isolation is effective at minimizing the peak isolator displacement at the base of the structure, while reducing peak interstory drifts and peak floor accelerations. Although multi-level seismic isolation is effective at reducing higher mode effects, currently no design guidelines exist for such systems. A central question for preliminary design of these multi-level rocking systems is the number, vertical location $(h_1, h_2, \dots)$ and hinge properties $(x_1, x_2, \dots)$ of the rocking joints (**Fig.1**).

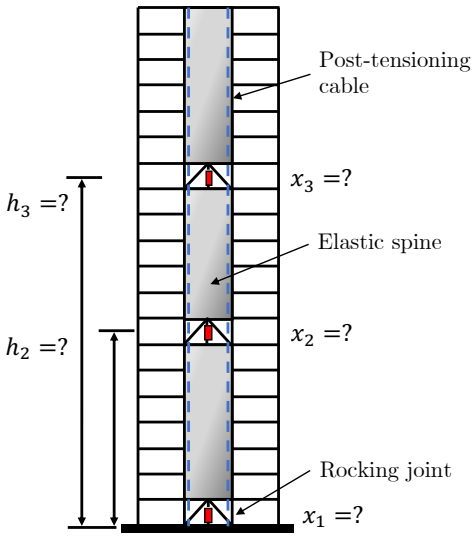

Fig. 1 – Stacked rocking system configuration

Simultaneously designing both the nonlinear articulated hinges and elastic spine is a difficult task due to the coupled nonlinear response and redistribution of internal forces from energy-dissipating elements. The

challenge is to control deformations while reducing seismic force demands by allowing multiple rocking sections. Previous research studies have examined the viability and seismic performance of stacked rocking systems but are often limited in scope. A more robust and exhaustive search of design parameters can be performed using mathematical programming. New simplified capacity design procedures, based on modified modal response spectrum analysis, have been introduced for single rocking systems [11], [12]. However, nonlinear dynamic analyses are necessary to adequately obtain structural response quantities for multi-level stacked rocking systems due to complex nonlinear dynamic behavior.

Structural optimization algorithms have been developed to determine optimal location and properties of dampers in earthquake-resistant structural systems devices such as retrofitting steel moment frames with fluid viscous dampers [13], or designing buckling-restrained braces in steel frames [14]. Non-gradient based techniques have also been used for the optimization, for instance, using a genetic algorithm, multi-level isolation was found to be effective at reducing large base isolator displacements and peak floor accelerations [15].

Stacked rocking systems are an effective seismic protection solution, which reduce higher mode effects in high-rise buildings through multi-level rocking hinges. However, designing the nonlinear rocking joints is a complicated task due to the nonlinear dynamic response of these systems and redistribution of inelastic seismic force demands. In this study, a gradient-based optimization framework, using selected nonlinear dynamic analyses from a set of hazard-consistent ground motion records, is developed for determining the number, vertical location and properties of nonlinear rocking joints along stacked rocking wall systems. The methodology is applied to an example 20-story stacked rocking wall system with dual hinges.

2. Numerical Modeling

2.1.OpenSees Nonlinear Model

The stacked rocking system is modeled in *OpenSees* [16] as a combination of elastic Timoshenko beams and self-centering springs as shown in **Fig.2**. The rocking spines are assumed to be RC wall sections, while the nonlinear dampers are buckling-restrained braces (BRBs). The spine is modeled as an elastic Timoshenko beams with both flexure and shear deformations using flexure and shear stiffnesses EI, GA. Lumped masses representing the weight of the rocking wall are placed at every story. A leaning column with tributary floor and roof masses is used to represent geometric nonlinear effects. Rocking hinges are introduced at every story using zero-length elements and the self-centering material with post-yield stiffness $\alpha = 0.05$ and energy-dissipation ratio $\beta = 0.8$, which constitutes a flag-shape hysteresis (**Fig. 2b**). The area of the BRB controls the initial stiffness and yield strength of the flag shape. A small fraction of the mass of the rocking wall is attributed to the top node of the hinge for numeric stability. The self-centering hinges are purely rotational while axial and shear effects are neglected by constraining the x and y-translational degrees of freedom to the bottom node of the elastic beam above.

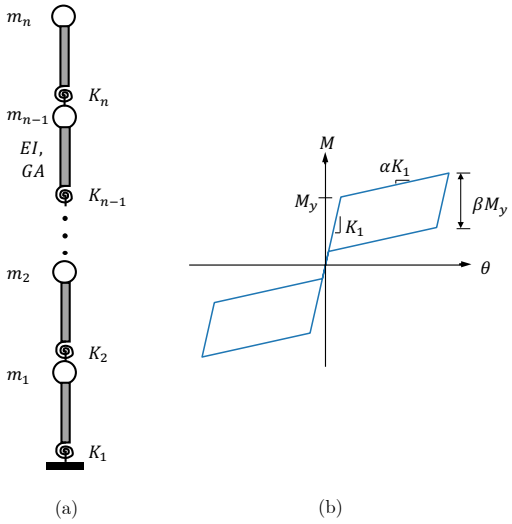

Fig. 2 - Numerical model (a) simplified stacked rocking model (b) self-centering flag-shape hysteresis

Since we assume that all the inelasticity is allocated to the hinges, this "stick-model" is deemed suitable for characterizing the seismic response of stacked rocking systems, compared to full fiber nonlinear element modeling [17]. In addition, the full distributed nonlinear model is computationally expensive, unnecessarily increasing the nonlinear dynamic analysis run time in the optimization process.

2.2.Nonlinear Dynamic Analyses

A suite of 50 ground motion records are selected from the PEER NGA West 2 database to represent a hazard-consistent set representing the MCE design spectrum with $Sa_s = 1.5$ s and $Sa_1 = 0.9$ s. The ground motions were selected by minimizing the pseudo-acceleration spectral ordinate error between the design spectrum and the median spectrum at periods $0.2\,T_1, 2T_1$ and $3T_1$, where $T_1 = 2.0$ s from ASCE7. In order to be hazard consistent with the chosen location of downtown San Francisco, several geophysical properties were matched. The rupture distance was set to the range of 5 to 50 km and the magnitude between 6.5 and 7.5 for a strike-slip fault mechanism. The maximum scale factor was set as 3 to not deviate the spectral shape. The shear wave velocity range was selected to represent a soil of type D, between 199 and 599 m/s. The response spectra for the record set for 5% damping is shown in **Fig. 3**. The goal of the design and optimization of the stacked rocking system is to target the median value of the response spectra. The implicit Newmark integration scheme was used with parameters $\beta = 0.25, \gamma = 0.5$ representing the average acceleration integration algorithm. The time step for the integration was initially set as half the time step in the record and decreased subsequently when encountering convergence issues.

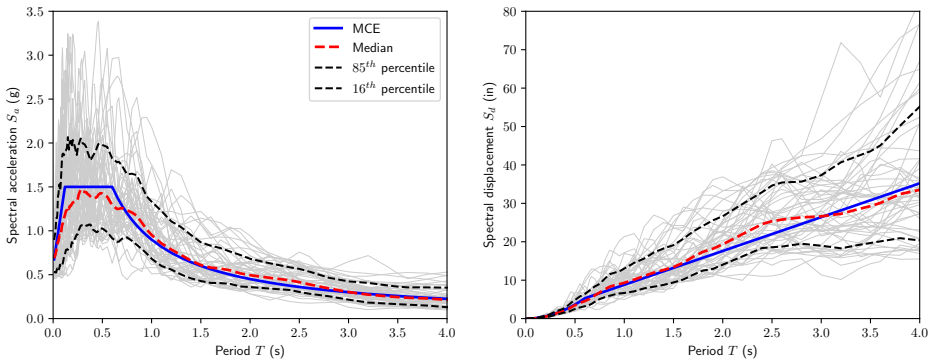

Fig. 3 - Response spectra for the suite of 50 ground motions and MCE design spectrum (a) pseudo-acceleration and (b) displacement

3. Optimization Framework

3.1. Problem Formulation

In order to accurately capture the rocking response of the stacked structure, nonlinear dynamic analyses will serve as the basis for the optimization. The goal of the optimization is to design the location and properties of the rocking interfaces for the median response under MCE level earthquake. The properties of the rocking hinges are directly controlled by the areas of the BRB dampers, which are the design variables in the optimization. By introducing nonlinear rocking planes, the aim is to reduce the cost of the elastic spine by curtailing peak force demands in the spine, which is measured by moment envelope. The objective function is the normalized integral of the overturning seismic moment demand along the height of the rocking spine. There are two constraints on: (1) the maximum drift of the stacked rocking system and (2) the rotation in each rocking hinge in order to prevent the BRBs from fracturing. The sizes of the BRBs are restricted by a lower and upper bound based on strength reduction tolerances. The optimization problem formulation is the following:

$$\begin{aligned} \text{minimize:} \quad & f(\boldsymbol{x}) = \frac{1}{M_y}\int_0^H M(\boldsymbol{x}, z)dz \\ \text{subject to:} \quad & g_0(\boldsymbol{x}) = d_{max}(\boldsymbol{x}) - \bar{d} \le 0 \\ & g_i(\boldsymbol{x}) = \theta_i(\boldsymbol{x}) - \bar{\theta} \le 0, \qquad \text{for } i = 1, \dots, N \\ & x_{min} \le x_j \le x_{max}, \qquad \text{for } j = 1, \dots, N_{DV} \end{aligned} \tag{1}$$

where $\boldsymbol{x}$ is the design variable, the vector of BRB areas, $M(\boldsymbol{x}, z)$ is the moment at elevation z, d_{max}, $\bar{d}$ are the maximum interstory drift and prescribed drift limit, θ_i, $\bar{\theta}$ are the hinge rotation at story i and prescribed rotation limit, x_{min}, x_{max} are the lower and upper bounds on the design variable and n is the number of stories and N_{DV} is the number of design variables. The integral of overturning moment is computed by summing the moments at each story level. The maximum interstory drifts are defined as:

$$d_{max} = \max\left\{\frac{|u_{i+1}(t) - u_i(t)|}{h_i}\right\} \tag{2}$$

where $u_i(t)$ is the displacement of floor i at time t, and h_i is the height of story i. The drift is constrained to a limit of 2.5%, according to Tall Building Initiative (TBI) guidelines under MCE level. Structural damage to the rocking spine is mitigated by constraining the story drifts, which serves as a global constraint. The prescribed rotation limit for the discrete hinges is obtained as: $\bar{\theta} = \mu\theta_y$, where μ is the BRB ductility ratio and θ_y is the rocking hinge yield rotation. A ductility ratio of μ=10 is used for this study based on statistical experimental evidence [18]. The yield displacement of the BRB is 5.0 mm, which leads to a yield rotation of $\theta_y = 0.1\,\%$ and a rotation limit of $\bar{\theta} = 1.0\,\%$. Although more complete fracture limit states such as cumulative plastic ductility or triaxial stress damage index [19] considering hysteretic behavior can be used, a deformation fracture capacity was deemed sufficient for the scope of this study.

3.2. Ground Motion Selection Algorithm

The goal of the optimization is to obtain the best design for the median response from a set of ground motions. However, computing all nonlinear dynamic responses at each optimization step is computationally intensive.

Indeed, each optimization step, using finite-difference for the estimation of the gradients, requires $(n_{DV}+1)n_{GM}$ nonlinear dynamic analyses, where n_{DV} is the number of design variables and n_{GM} is the number of ground motions. In order to speed-up the optimization, the median response can be approximated by carefully selecting one ground motion that best predicts the median. In this study, the "best median-predictor" ground motion is chosen based on minimizing the normalized relative sum errors of the engineering demand parameters, specifically interstory drifts and rotations of the active nonlinear hinges:

$$E(k) = E_d(k) + E_\theta(k) = \frac{1}{n}\sum_{i=1}^{n}\frac{\left|\overline{d_i} - d_i(k)\right|}{\overline{d_i}} + \frac{1}{n_{DV}}\sum_{j=1}^{n_{DV}}\frac{\left|\overline{\theta_j} - \theta_j(k)\right|}{\overline{\theta_j}} \tag{3}$$

where n, n_{DV} are the number of stories and design variables, $\overline{d_i}, d_i(k)$ are the median and individual response (k) interstory drifts at story i and $\overline{\theta_j}, \theta_j(k)$ are the median and individual response (k) hinge rotation of design hinge j. Only the design hinges are used for this error metric, since all the other stories will have zero hinge rotations.

3.3. Sequential Linear Programming (SLP)

The optimization problem is solved using a gradient-based optimization solver, sequential convex programming. Specifically, we will use first order information and thus implement a modified Sequential Linear Programming (SLP) solver [20]. Since the nonlinear dynamic response of the structure is not explicitly known in terms of the design variables, an iterative optimizer must be used. The objective function and constraints are linearized in terms of the design variables using a first order approximation as follows:

$$f(\boldsymbol{x}) \approx f(\boldsymbol{x}^k) + \nabla f(\boldsymbol{x}^k)(\boldsymbol{x} - \boldsymbol{x}^k) \tag{4}$$

where $\boldsymbol{x}^k$ is the current update point. The sensitivities are evaluated using the backwards finite-difference method. Since the linear approximations are only accurate in a neighborhood of the current update $\boldsymbol{x}^k$, a trust region is formed which controls the extent of the optimization step where:

$$\mathcal{T}(\boldsymbol{x}^k) = \{\boldsymbol{x} \mid |\boldsymbol{x} - \boldsymbol{x}^k| \leq \delta\} \tag{5}$$

where δ is the prescribed change limit, where the move limit is initially set as: $\delta = 0.10$. The move limit becomes smaller as the unfeasible domain is approached during the optimization. This is implemented in order to not overshoot and obtain an unfeasible design. Once the problem is linearized, the sub-optimization problem is solved using the standard linear programming (LP) solver. The optimization procedure is inspired by the Cutting-Plane Algorithm, where at each iteration an additional constraint is added to the original sub-problem [21]. The constraint that is the closest to the current design point is added. In addition, the constraints are evaluated and removed if deemed too conservative at successive iterations.

The modified SLP algorithm flowchart is summarized in **Fig.4**. The optimization is run until convergence is reached on the design variable $\|\Delta\boldsymbol{x}\|_2 \leq 0.001$ or a maximum number of iterations is reached. The function, constraints and sensitivities are evaluated using the peak response from the nonlinear dynamic analysis of the selected ground motion best median-predictor record $k^\star$. Using the finite-difference

approximations, the sub-optimization problem is solved using a standard LP solver. The update in the trust-region is made using the move limit. Finally, the optimized nonlinear damper sizes are determined once the algorithm converges.

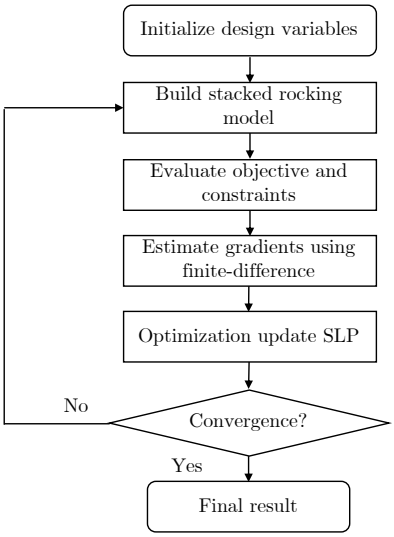

Fig. 4. SLP optimization algorithm flowchart

4. Results

4.1. High-Rise Building Case Study

A stacked rocking reinforced concrete wall prototype of 20 stories was designed for a site location in downtown San Francisco with soil type D. The building has story heights of 4.57 m and bay width of 9.14 m for the rocking wall. The post-tensioning cable are placed at the extremities of the width of the wall, while the buckling-restrained braced are centered at mid-bay. The maximum considered earthquake (MCE) level design spectral accelerations are $Sa_s = 1.5\ s$ and $Sa_1 = 0.9$ s for short and one second periods respectively. The tributary weights are 9,858 kN for the floors and 7,590 kN for the roof, including the weight of the wall. The building consists of four stacked rocking walls in each direction as lateral load-resisting systems. The stacked rocking wall properties are shown in **Table 1** along with the fundamental period obtained from ASCE 7. Since most of the inelasticity is expected to occur in the rocking hinges, the concrete wall is expected to undergo minor cracking with effective flexure and shear stiffnesses as $EI_{eff} = 0.75\,EI$ and $GA_{eff} = 0.75\,GA$, according to TBI guidelines for service loading. Buckling-restrained braced are used as the energy dissipation elements with grade A36 steel, a yield stress of $f_y = 248$ MPA, an expected yield stress factor of $R_y = 1.5$ and a core length factor of $LF = 2$.

Table 1 – 20-story stacked rocking wall properties

Model	H [m]	B [m]	GA_{eff} [kN]	EI_{eff} [kN-m2]	T_1 [s]
SR20	91.4	9.1	$4.37\ 10^7$	$2.01\ 10^9$	2.02

4.2. Design Space Exploration

In order to investigate the performance of the Sequential Linear Programing (SLP) optimization and ground motion selection routine, a dual stacked rocking case study is explored, referred to as SR20-2 for stacked

rocking of 20 stories and 2 hinges. The rocking hinges are located at the base (floor 1) and mid-height (floor 10) in order to reduce primarily the response from the first two modes. There are two design variables: the areas of the BRB in each rocking hinge, (x_1, x_2). The three constraints are (1) maximum drift limit to 2.5% (2) first rocking hinge rotation and (3) second rocking rotation both limited to 1.0%. In order to investigate the median response and ground motion selection routine, the full nonlinear surface of the design space is plotted in **Fig.5** showing both the objective function and maximum constraint median values. The response surface shows the median value for the set of 50 ground motion records, thus totalling 4,050 nonlinear dynamic analyses for the 20-story stacked rocking system.

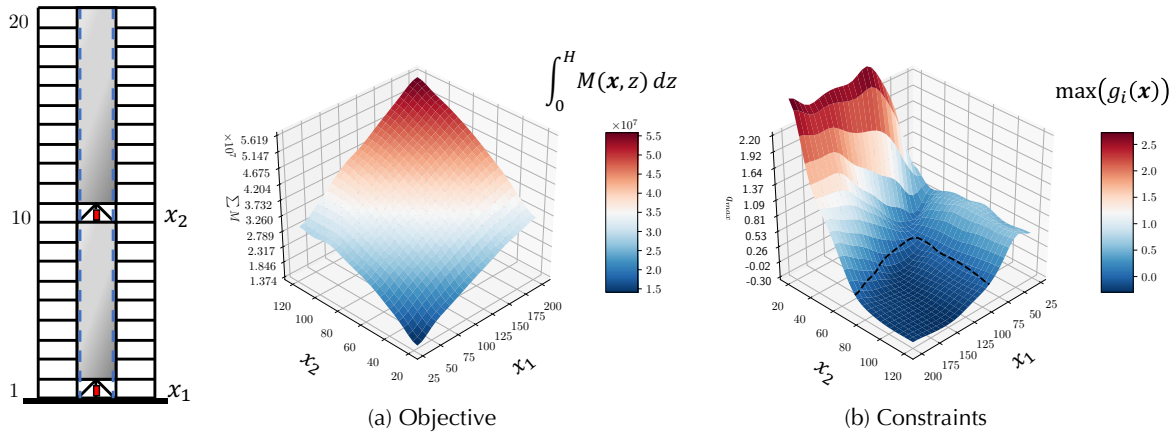

Fig. 5 – SR20-2 dual hinge stacked rocking optimization response surfaces

The objective function is smooth and can accurately be approximated by a surface plane, which is well suited for gradient-based optimization techniques such as SLP. In contrast, the constraints form a highly non-convex surface due to the complex nonlinear deformation behavior and coupled modal dynamics of the stacked rocking system. The challenge for the optimization algorithm is to clearly identify the feasible domain, since the global optimum is located on the boundary. From the design space exploration, the global optimum is $\boldsymbol{x}^\star = (82.3, 52.8)$ in^2 with both rotational hinge constraints active, while the drift limit constraint is inactive.

4.3. Ground Motion Selection

In order to find the best median prectitor ground motion record, the response of the dual hinge stacked system with the initial conditions of $\boldsymbol{x}_0 = (200, 120)$ in^2 is evaluated using all 50 ground motion records and the median response values are identified. **Table 2** shows the ground motion selection process based on the initial starting point. The records that lead to the closest response to the median response are shown for drift, hinge rotations and total error. Ground motion RSN6923-Darfield (GM #44) is the best predictor of the median response with a normalized error of 0.105. Indeed, GM #44 is the third best predictor for drift and second best predictor for hinge rotation. Some records are good predictors for drift, but poor predictos for hinge rotations and vice-versa.

Table 2 – Ground motion selection and median error predictions

Rank	Record (k)	E_d	Record (k)	E_θ	Record (k)	E
1	RSN5823 (31)	0.018	RSN5829 (34)	0.063	RSN6923 (44)	0.105
2	RSN725 (15)	0.028	RSN6923 (44)	0.075	RSN180 (8)	0.165
3	RSN6923 (44)	0.029	RSN5827 (47)	0.119	RSN6952 (47)	0.172

Fig.6 shows the nonlinear responses for the set of ground motion records including rocking hinge rotations, interstory drift, story shear and overturning moment for the initial conditions of $\boldsymbol{x}_0 = (200, 120)\ \text{in}^2$. Higher mode effects in the nonlinear reponse of the stacked rocking wall are apparent from the inverted S-shape pattern of the story shear forces and double curvature of the bending moment envelope. The interstory drift is a combination of the flexural and shear deformation of the two rocking sections in addition to the rocking hinge rotations. The median values and closest response (GM #44) are plotted for comparison. Since the ground motion record accuteraly estimates hinge rotations, interstory drifts as well as overturning moments, it will serve as the basis for the optimization.

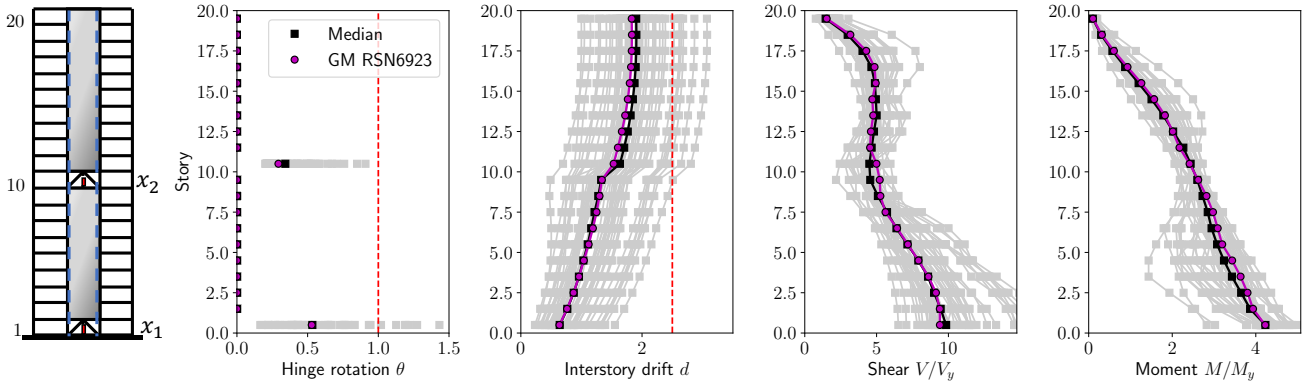

Figure 6 - SR20-2 initial nonlinear response $(x_1, x_2)_o = (200, 120)\ \text{in}^2$

4.4. SLP Optimization Results

The goal of the optimization procedure is to estimate the global optimum, considering the median response of the suite of ground motions, while using only the response of ground motion #44. Each function evaluation and sensitivity analysis consists of a costly nonlinear dynamic analysis. In this case we have two design variables (each damper size) and one ground motion, thus there are three nonlinear dynamic analyses for each optimization iteration. The initial starting point is chosen as $\boldsymbol{x}_o = (200, 120)\ \text{in}^2$. The optimization path and convergence history are shown in **Fig.7.** The SLP optimization convergences in 13 iterations or the equivalent of 39 nonlinear time history analyses. The descent path is that of steepest descent until the design iterations hits the constraint boundary for the rotation of the second hinge. The initial and optimized parameters are shown in **Table 3**. The optimization terminates at $\boldsymbol{x}^{\star}_{SLP} = (96.0, 54.6)\ \text{in}^2$ with a normalized sum of moments of 27.2, which corresponds to a reduction of 42% in overturning moments, as compared to the original design. The peak drift is 1.87%, first rotation is 1.10% and second hinge rotation is 0.96%. Thus, the SLP optimization correctly approximated the optimum from record GM #44. Considering the median response of all 50 ground motions, the true global optimum is $\boldsymbol{x}^{\star}_{SLP} = (82.3, 52.8)\ \text{in}^2$ However, considering only one ground motions, we were able to estimate the global optimum in solely 39 nonlinear dynamic analysis compared to the 4,050 required to obtain the complete design space.

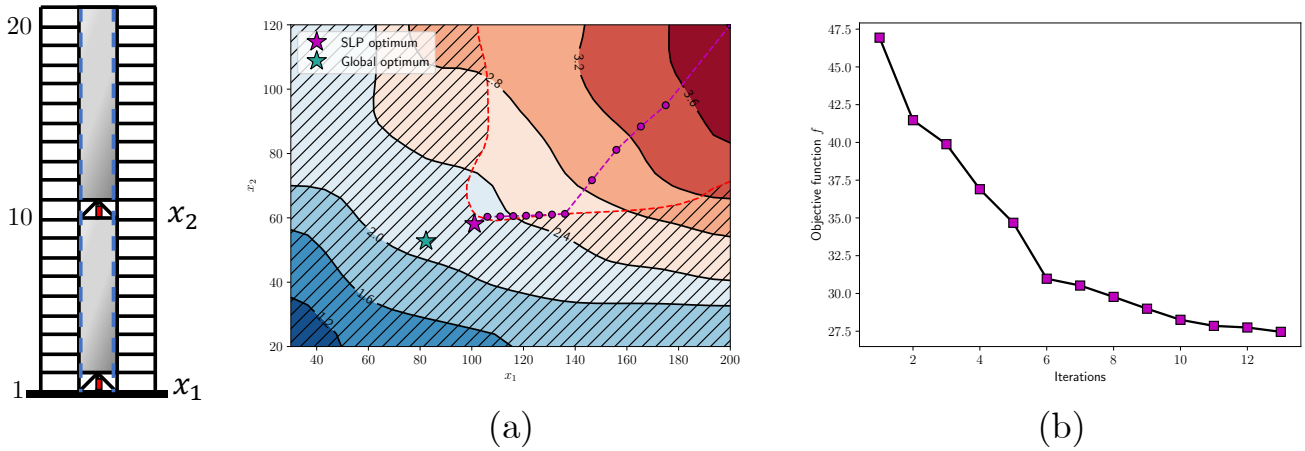

Figure 7 – SR20-2 SLP optimization results (a) objective contour space evolution and (b) convergence history

Table 3 – SR20-2 SLP optimization results

Design	x_1 [in^2]	x_2 [in^2]	f=$\sum M/M_y$ [-]	d_{max} [%]	θ_1 [%]	θ_2 [%]
Initial	200	120	46.9	1.83 %	0.53 %	0.29 %
SLP (GM 44)	96	54.6	27.2	1.87 %	1.10 %	0.96 %

Finally, **Table 4** highlights the various optimized designs considering only 1 hinge or 2 hinges. Both single and dual hinge stacked rocking systems are constrained to a 1% hinge rotational limit. Introducing a hinge at midheight yields lower story shear forces and overturning moments, but higher peak drift, from 1.72% to 1.87%. Thus, adding rocking hinges reduces force demands in the elastic spine but increases the flexibility and thus deformiation of the earthquake resistant structural system.

Table 4 – Multi-hinge parametric design exploration

Model	θ_{max}	d_{max}	$\sum V$	$\sum M$
SR20-1 (1 hinge)	1.0 %	1.72 %	92.4	33.4
SR20-2 (2 hinges)	0.97 %	1.87 %	88.2	27.2

5. Conclusion

A novel optimization framework was introduced for reducing seismic force demands, while maintaining drift and rotational constraints on stacked rocking systems for high-rise buildings. A modified sequential linear programming (SLP) algorithm was developed to solve the optimization problem. A case study high-rise building prototype of 20 stories with multi-level rocking walls was investigated considering two hinges (SR20-2), one at the base and one at mid-height. The design exploration space for the dual hinge case (SR20-2) served as a basis for finding and evaluating the median-predictor ground motion. This ground motion (GM#44), was in turn used to efficiently conduct the SLP optimization. The main findings of this study are highlighted below:

- The SLP optimization, conducted with the best median-predictor ground motion, GM #44, chosen using the nonlinear responses from the initial design, estimates relatively accurately the true global optimum considering the true median of all 50 ground motion records. The SLP optimization converged with only

13 iterations or 39 nonlinear dynamic analyses, compared to the exhaustive search of 4,050 nonlinear dynamic analyses.

- The optimized dual stacked rocking system reduces 30% story shear forces and 42% overturning moments compared to the initial design with a peak drift of 1.87% below the 2.5% prescribed limit.

The authors are currently investigating the extension of the proposed SLP optimization for a stacked rocking system with n-arbitrary hinges at every story. The goal of the optimization framework is to be able to determine not only the properties of the rocking hinges, but also their vertical locations.

6. Acknowledgments

The material and findings in this paper are based upon work supported by the National Science Foundation Graduate Research Fellowship under Grant No. DGE-114747, the Achievement Reward for College Scientists Scholar Fellowship and the James M. Gere Fellowship. The authors would also like to thank Glaucio Paulino, Jack Baker and researchers of the Blume Earthquake Engineering Center at Stanford for valuable insights and contributions.

7. References

[1] G. G. Deierlein, H. Krawinkler, X. Ma, M. Eatherton, J. Hajjar, T. Takeuchi, K. Kasai, M. Midorikawa, "Earthquake resilient steel braced frames with controlled rocking and energy dissipating fuses," *Steel Constr.*, vol. 4, no. 3, pp. 171–175, Aug. 2011.

[2] D. J. Marriott, S. Pampanin, A. Palermo, and D. Bull, "Shake-table testing of hybrid post-tensioned precast wall systems with alternative dissipating solutions," *2008 New Zeal. Soc. Earthq. Eng.*, no. 39, pp. 90–103, 2008.

[3] Z. Jin, S. Pei, H. Blomgren, and J. Powers, "Simplified Mechanistic Model for Seismic Response Prediction of Coupled Cross-Laminated Timber Rocking Walls," *J. Struct. Eng.*, vol. 145, no. 2, p. 04018253, 2018.

[4] M. R. Eatherton, "Large-scale cyclic and hybrid simulation testing and development of a controlled-rocking steel building system with replaceable fuses," 2010.

[5] L. Wiebe and C. Christopoulos, "Mitigation of higher mode effects in base-rocking systems by using multiple rocking sections," *J. Earthq. Eng.*, vol. 13, no. 1 SUPPL. 1, pp. 83–108, 2009.

[6] M. Khanmohammadi and S. Heydari, "Seismic behavior improvement of reinforced concrete shear wall buildings using multiple rocking systems," *Eng. Struct.*, vol. 100, pp. 577–589, 2015.

[7] L. Wiebe and C. Christopoulos, "Performance-Based Seismic Design of Controlled Rocking Steel Braced Frames. II: Design of Capacity-Protected Elements," *J. Struct. Eng.*, vol. 141, no. 9, p. 04014227, 2014.

[8] D. S. Pilon, A. Palermo, F. Sarti, and A. Salenikovich, "Benefits of multiple rocking segments for CLT and LVL Pres-Lam wall systems," *Soil Dyn. Earthq. Eng.*, 2019.

[9] X. Chen, T. Takeuchi, and R. Matsui, "Seismic performance and evaluation of controlled spine frames applied in high-rise buildings," *Earthq. Spectra*, vol. 34, no. 3, pp. 1431–1458, 2018.

[10] M. C. Phocas and G. Pamboris, "Multi-storey Structures with Seismic Isolation at Storey-Levels," Springer, Cham, 2017, pp. 261–284.

[11] T. C. Steele and L. D. A. Wiebe, "Dynamic and equivalent static procedures for capacity design of controlled rocking steel braced frames," *Earthq. Eng. Struct. Dyn.*, 2016.

[12] A. Martin, G. G. Deierlein, and X. Ma, "Capacity Design Procedure for Rocking Braced Frames Using Modified Modal Superposition Method," *J. Struct. Eng.*, 145-(6), 04019041, 2019.

[13] S. Wang, "Enhancing Seismic Performance of Tall Buildings by Optimal Design of Supplemental Energy-Dissipation Devices," 2017.

[14] F. Farhat, S. Nakamura, and K. Takahashi, "Application of genetic algorithm to optimization of buckling restrained braces for seismic upgrading of existing structures," *Comput. Struct.*, vol. 87, no. 1–2, pp. 110–119, Jan. 2009.

[15] D. C. Charmpis, P. Komodromos, and M. C. Phocas, "Optimized earthquake response of multi-storey buildings with seismic isolation at various elevations," *Earthq. Eng. Struct. Dyn.*, 2012.

[16] F. McKenna, "OpenSees: A framework for earthquake engineering simulation," *Comput. Sci. Eng.*, 2011.

[17] J. S. Pugh, L. N. Lowes, and D. E. Lehman, "Nonlinear line-element modeling of flexural reinforced concrete walls," *Eng. Struct.*, vol. 104, pp. 174–192, Dec. 2015.

[18] C. J. Black, N. Makris, and I. D. Aiken, "Component Testing, Seismic Evaluation and Characterization of Buckling-Restrained Braces," *J. Struct. Eng.*, vol. 130, no. 6, pp. 880–894, 2004.

[19] M. Terashima, "Ductile fracture simulation and risk quantification of buckling-restrained braces under earthquakes," Doctoral Dissertation, Stanford University, 2018.

[20] P. W. Christensen and A. Klarbring, "An introduction to structural optimization," *Solid Mech. its Appl.*, 2008.

[21] R. Levy and O. Lavan, "Fully stressed design of passive controllers in framed structures for seismic loadings," *Struct. Multidiscip. Optim.*, vol. 32, no. 6, pp. 485–498, 2006.

